Influence of Acetate Buffers and Metal Ions on Ketonization Rates of Enolpyruvate: A Further Test of the Marcus Function

Barbara A. Miller and Daniel L. Leussing*

Contribution from the Department of Chemistry, The Ohio State University, Columbus, Ohio 43210. *Received February 19, 1985*

Abstract: Enolpyruvate, **1** (HEP^-), had been generated by enzymatically cleaving phosphate from PEP, and the rates of ketonization were determined in acetate buffers in the absence and presence of divalent metal ions, Mg(II), Mn(II), and Cu(II). Second-order metal ion independent catalytic ketonization rate constants are $k_{HEP}^{H} = 1.7 \times 10^2\ M^{-1}\ s^{-1}$, $k_{HEP}^{HOAc} = 0.13\ M^{-1}\ s^{-1}$, and $k_{HEP}^{OAc} = 0.65\ M^{-1}\ s^{-1}$. Third-order metal-dependent rate constants for cooperative catalysis with ^-OAc are $9 \times 10^2\ M^{-2}\ s^{-1}$ (Mg), $4.0 \times 10^3\ M^{-2}\ s^{-1}$ (Mn), and $3.0 \times 10^5\ M^{-2}\ s^{-1}$ (Cu). Cu(II) also displays a cooperative pathway with HOAc which has a surprisingly high rate constant, $4.7 \times 10^5\ M^{-2}\ s^{-1}$. The Marcus equation with an intrinsic barrier of 13.5 kcal mol^{-1} was found to account for these rates, as well as those previously reported for the ketonization of vinyl alcohol[47] and oxalacetate.[13,35,49] The results support an earlier conclusion[13] that complexing to a metal ion does not influence the height of the intrinsic barrier. The rate constant predicted from Marcus theory for the direct attack of HOAc on $Cu(HEP)^+$ is several orders of magnitude less than that observed; however, the constant calculated for the attack of H^+ on Cu(HEP)(OAc), accompanied by transfer of the proton from enol to the bound OAc^-, is in very good agreement with the observed value.

Enolpyruvate,[1] **1**, HEP^-, is a high-energy substance which may be an active intermediate in a number of important biological transformations. Recent studies[2-4] have shown HEP^- to be a substrate for reactions catalyzed by pyruvate kinase (PEP + ADP $\rightleftharpoons$ ATP + PYR^-, PEP = phosphoenolpyruvate, PYR^- = pyruvate), transcarboxylase ($^-O_2CCH(CH_3)CO_2^- + CH_3COCO_2^- \rightleftharpoons CH_3CH_2CO_2^- + {}^-O_2CCH_2COCO_2^-$), and pyruvate carboxylase ($CH_3COCO_2^- + CO_2 \rightleftharpoons {}^-O_2CCH_2COCO_2^-$). HEP^- also may be the reactive component in the first step of the Shikimic acid pathway through which plants, fungi, and bacteria synthesize aromatic compounds[5] (erythrose 4-phosphate + PEP $\rightleftharpoons$ P_i + 3-deoxyheptulosonic acid 7-phosphate). An early study demonstrated that the 3,3-dimethyl derivative of enolpyruvate is produced as an intermediate in the decarboxylation of 3,3-dimethyl oxalacetate,[6] and subsequent evidence for the formation of enolpyruvate during the decarboxylation of oxalacetate has been obtained.[7] Although enolpyruvate ketonizes rapidly relative to its rate of generation, it can be trapped by pyruvate, oxalacetate, or erythrose 4-phosphate to produce pyruvate dimer,[8-10] formyl citrate,[11] or the phosphorylated deoxyheptulosonic acid.[12]

In spite of its biological importance, difficulties in generating HEP^- in detectable concentrations have impeded studies of its behavior. In the present investigation, we have exploited a method used by Rose[2-4] in which HEP^- is generated enzymatically by hydrolyzing PEP. Rates of ketonization were studied in acetate buffers in the presence, or absence, of complexing metal ions, Mg(II), Mn(II), and Cu(II). Ketonization competes with other reactions of HEP^- and therefore must be studied as a first step in elucidating the general chemistry of this substance. Of significant interest is information to be gained concerning cooperativity effects between metal ions and general acid or general base catalysts. Recently, it has been shown[13] that enhanced catalysis effected by Mg(II) on the enolization, hydration, and decarboxylation rates of oxalacetate can be quantitatively described simply by taking into account the effect of reactant and product complexing on the standard free-energy term of the Marcus equation (eq 1).[14]

$$\Delta G^{\ddagger} = \Delta G^{\ddagger}_0 + \Delta G^{\circ}/2 + (\Delta G^{\circ})^2/16\Delta G^{\ddagger}_0 \qquad (1)$$

In (1), $\Delta G^{\ddagger}$ is the observed activation barrier related to the rate constant according to eq 2, ΔG° is the standard free-energy change for the rate limiting step, and $\Delta G^{\ddagger}_0$ is the "intrinsic" barrier for the reaction at $\Delta G^{\circ} = 0$.

$$\Delta G^{\ddagger} = -RT \ln k + RT \ln (2.084 \times 10^{10} T) \qquad (2)$$

Kresge[15] has discussed the success of eq 1 in accounting for the nonlinearity observed in Brønsted plots for the rates of general base catalyzed enolization reactions.[16,17] More recently, Albery[18-20] has demonstrated that the six rate constants found for the enolization of acetone in acetate buffers, k_H, k_{OH}, k_{H_2O}, k_{HOAc}, k_{OAc}, and one for a cross term, $k_{HOAc,OAC}$, have values which are related by eq 1. An important result is the demonstration that $\Delta G^{\ddagger}_0$ is insensitive to changes in the groups covalently bonded to the carbonyl carbon atom.[15,17-19] One conclusion drawn in ref 13 is that coordination of oxalacetate to Mg(II) also has no influence on the intrinsic barrier. Because it is often possible to estimate ΔG° for a particular coordination environment about a metal ion using the extensive information that is available in the literature, a powerful, yet simple, means of predicting rate constants for postulated metal ion dependent reaction paths ap-

(1) Abbreviations: ADP, adenosine diphosphate; ATP, adenosine triphosphate; EP^{2-}, the enolate of pyruvate; HEP^-, enolpyruvate; H_2EP, protonated enolpyruvate; OAc^-, acetate; $OXAC^{2-}$, oxalacetate; P-AP, white potato phosphatase; PEP, phosphoenolpyruvate; P_i, inorganic phosphate; PYR^-, pyruvate; β_{MX}, the stability constant of an MX complex, M + X → MX.

(2) Kuo, D. J.; Rose, I. A. *J. Am. Chem. Soc.* **1978**, *100*, 6288.
(3) Kuo, D. J.; O'Connell, Rose, I. A. *J. Am. Chem. Soc.* **1979**, *101*, 5025.
(4) Kuo, D. J.; Rose, I. A. *J. Am. Chem. Soc.* **1982**, *104*, 3235.
(5) Haslam, E. "The Shikimate Pathway"; Halsted Press, Wiley: New York, 1974. Weiss, U.; Edwards, J. M. "The Biosynthesis of Aromatic Compounds"; Wiley: New York, 1980.
(6) Steinberger, R.; Westheimer, F. H. *J. Am. Chem. Soc.* **1951**, *73*, 439.
(7) For recent reviews, see: (a) Hay, R. W. "Metal Ions in Biological Systems"; Sigel, H., Ed.; Marcel Dekker: New York, 1976; Vol. 5. (b) Leussing, D. L. "Advances in Inorganic Biochemistry"; Eichhorn, G. L., Marzilli, L. G., Eds.; Elsevier Biomedical: New York, 1982; Vol. 4.
(8) Lillis, B.; Leussing, D. L. *Chem. Commun.* **1975**, 397.
(9) Tallman, D. E.; Leussing, D. L. *J. Am. Chem. Soc.* **1969**, *91*, 6253, 6256.
(10) Gallo, A. A.; Sable, H. Z. *Biochim. Biophys. Acta* **1973**, *303*, 443.
(11) Wiley, R. H.; Kim, K.-S. *J. Org. Chem.* **1973**, *38*, 3582.
(12) Herrmann, K. M.; Poling, M. D. *J. Biol. Chem.* **1975**, *17*, 6817.
(13) Leussing, D. L.; Emly, M. *J. Am. Chem. Soc.* **1984**, *106*, 443.
(14) Marcus, R. A. *J. Phys. Chem.* **1968**, *72*, 891; *J. Am. Chem. Soc.* **1969**, *91*, 7224.
(15) (a) Kresge, A. J. *Acc. Chem. Res.* **1975**, *8*, 354. (b) *Chem. Soc. Rev.* **1973**, *2*, 475. (c) Chiang, Y.; Kresge, A. J.; Walsh, P. A. *J. Am. Chem. Soc.* **1982**, *104*, 6122-6123.
(16) Bell, R. P. "The Proton in Chemistry", 2nd ed.; Cornell University Press: Ithaca, NY, 1973.
(17) Toullec, J. *Adv. Phys. Org. Chem.* **1982**, *18*, 1-77.
(18) Albery, W. J. *Annu. Rev. Phys. Chem.* **1980**, *31*, 227.
(19) Albery, W. J.; Gelles, J. S. *J. Chem. Soc., Faraday Trans. 1* **1982**, *78*, 1569-1578.
(20) Albery, W. J. *J. Chem. Soc., Faraday Trans 1*, **1982**, *78*, 1579.

0002-7863/85/1507-7146$01.50/0

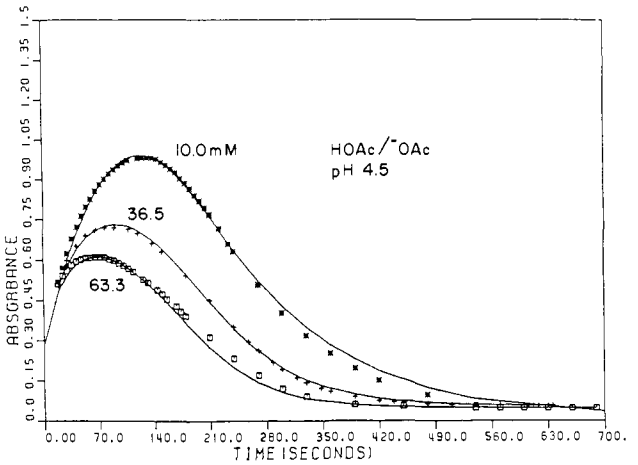

Figure 1. Influence of total acetate on the ketonization rates of enolpyruvate. I = 0.1 (KCl). The solid lines are theoretical.

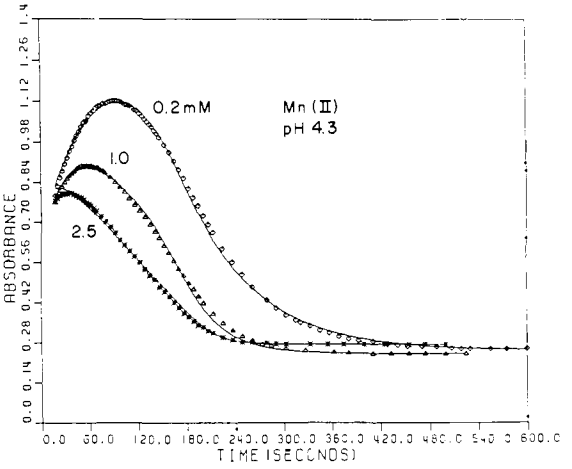

Figure 2. Influence of Mn(II) on the ketonization rates of enolpyruvate. Total acetate = 0.0199 M. I = 0.10 (KCl). The solid lines are theoretical.

pears to be at hand. Although the intrinsic barrier for the decarboxylation of ZnOXAC was found to be the same as that determined for $OXAC^{2-}$ and MgOXAC, further experimental support for this discovery is needed. In the present investigation, that support has been obtained.

Experimental Section

The monopotassium salt of PEP and the sodium salt of pyruvate were obtained from Sigma Chemical Co. and used without further purification. The purities were checked by using a coupled assay with pyruvate kinase and lactate dehydrogenase. Acid phosphatase from white potatoes, P-AP (Sigma), was purified by using Sephadex G-150 gel permeation chromatography.[21] Appropriate fractions were pooled, concentrated by using an Amicon high-pressure ultrafiltration membrane, frozen in liquid nitrogen, and stored at ~70 °C.

All kinetic and equilibrium measurements were made at 25 °C, I = 0.1 (KCl). The protonation constants of PEP were determined potentiometrically with use of a Radiometer Model 26 pH meter: $pK_{1a}^{H_2PEP}$ = 3.45 ± 0.04, pK_{2a}^{HPEP} = 6.14 ± 0.05. Wold and Ballou[22] report values of 3.4 and 6.35 for the cyclohexylammonium salt. Molar absorptivities of the PEP species and PYR^- were determined by using a Gilford Model 250 spectrophotometer. At 235-nm values of 2380 (PEP^{2-}), 936 ($HPEP^-$), 1380 (H_2PEP), and 460 (PYR^-) M^{-1} cm^{-1} were obtained.

All kinetic determinations were performed spectrophotometrically. The Gilford spectrophotometer was interfaced to an Apple II Plus computer equipped with a DAS Model 5 A/D converter for data acquisition, digitization, and storage. The wavelength monitored, 235 nm, is not that reported for the HEP^- absorbance maximum, 230 nm,[3] but a slightly longer wavelength was chosen to reduce the background absorbance of the enzyme and, thereby, to ensure that stray light effects did not introduce deviations from Beer's law.

Each kinetic determination was initiated by the addition of 0.5 mL of a buffered PEP solution to 1.05 mL of a solution of potato acid phosphatase in the same buffer. The concentrations chosen for the final series of runs were 1.0 mM PEP and 1~2 × 10^{-6} M enzyme. Series of experiments were performed at given buffer ratios with varying total buffer concentrations. The pH ranged from 4.0 to 5.5. The influence of Mg(II), Mn(II), and Cu(II) was examined by adding salts of these metal ions to the enzyme solutions prior to adding PEP. Millimolar concentrations of Mg(II) (0.5~6 mM) and Mn(II) (0.2~2.5 mM) were found to furnish useful rate increases, but the catalytic effect of Cu(II) was found to be so large that only in the concentration range 1.0~15 × 10^{-6} M Cu(II) were useful ketonization rates obtained. At higher concentrations, the rate of PEP ketonization became so fast that the rate of generation of pyruvate was determined by the rate of which the enzyme cleaved PEP. At the metal ion concentrations employed, complexing of PEP[22] and metal ion catalysis of PEP hydrolysis[23] are negligible.

At 235 nm, the hydrolysis of PEP is accompanied by an absorbance increase arising from the appearance of HEP^-. As the PEP is depleted and HEP^- is converted to pyruvate, the absorbance decreases to a final value. Data points from representative absorbance–time curves obtained by using 0.50-cm cells arre shown plotted in Figure 1 for metal-free solutions, and in Figure 2 for solutions to which Mn(II) was added.

Results

Determination of the Ketonization Rate Constants. In agreement with Rose's results,[2-4] the dependence of the rates on reactant concentrations was found to conform to the sequence

$$PEP + P\text{-}AP \underset{}{\overset{K_e}{\rightleftharpoons}} PEP\cdot P\text{-}AP \xrightarrow{k_e} HEP^- + P_i + P\text{-}AP \quad (3)$$

$$HEP^- \xrightarrow{k_{keto}} PYR^- \quad (4)$$

Reactions 3 and 4 lead to the rate equations

$$\frac{d[HEP]}{dt} = k_e[PEP\cdot P\text{-}AP] - k_{keto}[HEP^-] = \frac{k_e K_e[PEP][P\text{-}AP]_{tot}}{1 + K_e[PEP]} - k_{keto}[HEP^-] \quad (5)$$

$$\frac{d[PYR^-]}{dt} = k_{keto}[HEP^-] \quad (6)$$

Absorbance at time t is given by

$$A_t = \epsilon_{PEP}[PEP] + \epsilon_{HEP}[HEP^-] + \epsilon_{PYR}[PYR^-] + A_{bg} \quad (7)$$

The combined enzyme and background absorbance, A_{bg}, is time-dependent.

The values of ϵ_{PEP}, ϵ_{PYR}, and A_{bg} are known independently; thus, four parameters, two describing enzyme activity, k_e and K_e, and two pertaining to HEP, k_{keto} and ϵ_{HEP}, are unknown and must be evaluated from the absorbance–time curves. Rose et al.[2-4] have described a method that applies to the situation where $K_e[PEP] \gg 1$, i.e., where the enzyme rate is constant over the time interval of interest. Preliminary experiments suggested that under certain of our reaction conditions, K_e may be as low as about 10^4 M^{-1} and, therefore, may be too small in some cases to maintain an essentially constant enzyme rate throughout the reaction. In order to obviate errors from this source, a nonlinear curve-fitting procedure based on the numerical integration of eq 5 and 6 was developed. Values of the unknown parameters were assumed for the initial concentrations pertaining to a given experiment, and a theoretical absorbance–time curve was calculated by using the Gear algorithm for numerical integration.[24] The sum square of the differences between the observed and calculated curves was obtained. The unknowns were varied, and a search for the best fit of the calculated to observed absorbance–time curve was made by using the set of nonlinear curve-fitting procedures incorporated at CERN into the package MINUIT.[25]

Preliminary experiments in which PEP and enzyme concentrations were varied demonstrated that values of k_{keto} and ϵ_{HEP}

(21) Miller, B. A. Ph.D. Thesis, The Ohio State University, Columbus, OH, 1984.
(22) Wold, F.; Ballou, C. E. *J. Biol. Chem.* **1957**, *227*, 301.
(23) Benkovic, S. J.; Schray, K. J. *Biochemistry* **1968**, *7*, 4097~4102.
(24) Gear, C. W. *Commun. ACM.* **1971**, *14*, 185-190.
(25) James, F.; Roos, M. *Comput. Phys. Commun.* **1975**, *10*, 343-367.

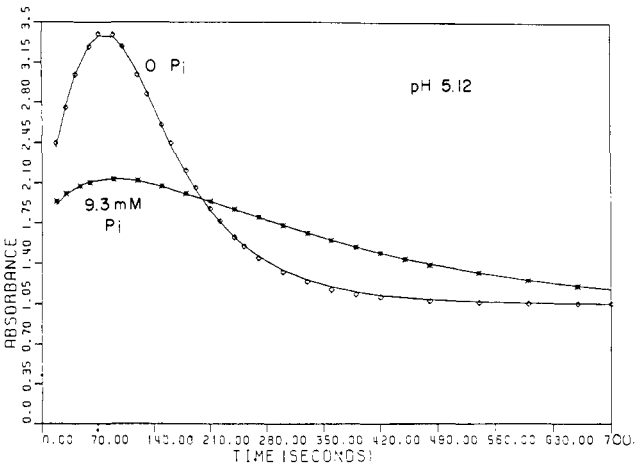

Figure 3. Inhibition of enolpyruvate generation by added phosphate. Total acetate = 0.025 M. $I = 0.1$ (KCl). The solid lines are theoretical.

Table I. Phosphate Inhibition of White Potato Acid Phosphatase

pH	log K_p	ref	pH	log K_p	ref
7.2	3.66	25	5.0	3.08	29
7.0	3.60	26	5.0	3.08	*a*
7.0	3.38	28	4.5	2.88	*a*
5.3	2.74	27	4.0	2.40	*a*

[a] This work.

are independent of these concentrations as long as enzyme activity was sufficient that PEP hydrolysis rates were not very slow with respect to ketonization.

Acid phosphatase is known to be inhibited by free phosphate,[26-30] and very minor deviations of the calculated curves from the observed curves were traced to this source. The influence of added phosphate on the rates is shown in Figure 3. Curve A with no added phosphate is seen to have a higher and sharper maximum and to reach the infinity absorbance sooner than curve B with 5.9 mM added phosphate. A value of K_p, eq 8, was obtained by fitting calculated curves to experimental curves collected by using 0 to 12 mM added phosphate. Values of K_p determined here together

$$\text{P-AP} + \text{P} \overset{K_p}{\rightleftharpoons} \text{PP-AP} \qquad (8)$$

with values reported in the literature are given in Table I. A slight increase in k_{keto} at the higher inhibitor concentrations indicated phosphate-catalyzed ketonization. The effect was found to be small enough that the influence of k_{keto} of the free phosphate liberated during the hydrolysis of 1 mM PEP could be safely neglected.

For the final computations, theoretical absorbance–time curves were simultaneously fit to all the observed curves obtained from the series of buffer dilution experiments at a given pH. The number of unknowns to be determined was reduced by using a common value of ϵ_{HEP} and replacing k_{keto} by the sum of buffer-independent and buffer-dependent terms (eq 9).

$$k_{keto} = k' + k''[\text{OAc}]_{tot} \qquad (9)$$

The value of ϵ_{HEP} was found to be 4.4×10^3 M^{-1} cm^{-1} in the region pH 4.5–5.5. At pH 4.0, the nominal value increased to 5.4×10^3, owing to the presence of an appreciable amount of H_2EP. From the spectrum presented by Rose[3] in D_2O, pD 5.0, ϵ_{HEP} is estimated to be about 3×10^3 M^{-1} cm^{-1}.

The solid lines drawn in Figures 1–3 represents the traces of the theoretical curves which had been calculated by using the "best" values found for the unknown parameters. Typical relative standard deviations in these parameters were indicated to be about 10% for ϵ_{HEP} and 15% for k' and k''. Reproduction of the observed spectral features is seen to have been achieved. In particular, excellent agreement has been obtained in the region of the maxima, the heights and positions of which are highly sensitive to the reaction rates. We have not been able to account for the somewhat larger deviations noted in Figure 1 in the regions where HEP^- and PEP become depleted.

Equilibrium Constants. The values of the equilibrium constants employed to analyze the results are presented in Table II. A number of the values have been determined experimentally, but those involving reactive enolpyruvate, or species which exist under experimentally difficult conditions, were obtained from estimates. For H_2EP, $pK_{1a} = 3.7$ ($CH_2{=}CH(CO_2H)OH \rightleftharpoons CH_2 = CH(CO_2^-)OH + H^+$) was calculated by using the Charton equation for the acidities of acrylic acids,[31,32] taking $\sigma_{meta} = 0.13$. Guthrie[33] has estimated the pK_a of vinyl alcohol to be 11.1, and Emly[34,35] has determined pK_{3a} of the enol form of oxalacetate to be 12.8, a value slightly higher than that obtained by Tate,[36] who used an erroneous extinction coefficient.[37] Kresge[15c] has measured the pK_a of the enol of isobutyraldehyde to be 11.63, in very good agreement with an estimate made by Guthrie.[33] We have assumed a value for HEP^- between those for vinyl alcohol and $OXAC_{enol}^{2-}$, $pK_{2a} \approx 12.0$ for $CH_2{=}C(CO_2^-)OH \rightleftharpoons CH_2{=}C(CO_2^-)O^- + H^+$. Earlier,[13] the stability constants of M^{II}–EP^{2-} complexes, β_{MEP}, were estimated by analogy from the reported stabilities of oxalacetate complexes; however, in the present work, it was deemed important to evaluate these constants directly from independent experimental data. According to the Marcus equation, the rate of decarboxylation of an oxalacetate complex is a function of the stability of the MEP complex which is produced; therefore, a way is provided for evaluating the β_{MEP} from decarboxylation data. The details of the calculations are provided below.

The stabilities of the enol complexes, $M(HEP)^+$, were estimated by assuming that a given complexing metal ion has the same *relative* influence on the pyruvate enol/keto ratio as it has on the oxalacetate enol/keto ratio, i.e., $K_{enol}^{MPYR}/K_{enol}^{MOXAC} = K_{enol}^{PYR}/K_{enol}^{OXAC}$, where K_{enol}^{X} is the constant for the equilibrium, $X_{keto} \rightleftharpoons X_{enol}$. This assumption leads to the simple relationship, $\beta_{MHEP} = \beta_{MOXAC(enol)}\beta_{MPYR}/\beta_{MOXAC(keto)}$. Although, this assumption is plausible, it must be noted that it has not been experimentally verified. The calculated magnitudes of the β_{MHEP} provide the important qualitative information that although the HEP^- complexes may be kinetically quite active, the actual fraction of HEP^- present as complex in any experiment was small. This made it possible when analyzing the kinetic results for cooperative metal ion–general base catalysis to employ a reaction path, path III, which does not require knowledge of the β_{MHEP}.

Estimates required to analyze acid-catalyzed rates also have large uncertainties. The pK_a of $HPYR^{\pm}$ ($CH_3C(CO_2^-){=}OH^+ \rightleftharpoons CH_3C(CO_2^-){=}O + H^+$) was taken to be −5.0 assuming that $HPYR^{\pm}$ should be somewhat less acidic than the conjugate acid of acetone, $(CH_3)_2C{=}OH^+$, for which Albery[20] and Hine[38] have estimated values of −7.7 and −6.0. Cox[39] gives values of −5.37 and −2.0 for the ionization constants of Hacetone$^+$ and an outer-sphere association complex, $^+H_3O\cdots$acetone. The stability constant of $Cu(HPYR^{\pm})^{2+}$, $CH_3C(OH^+)CO_2^-\cdots Cu^{2+}$ was assumed to be $10^{0.5}$ M^{-1}, the same as that determined[40] for $Cu(Hserine^{\pm})^{2+}$,

(26) Duggleby, R. G.; Morrison, J. F. *Biochem. Biophys. Acta* **1977**, *481*, 297.
(27) Hsu, R. Y.; Cleland, W. W.; Anderson, L. *Biochemistry* **1966**, *5*, 799.
(28) Jorgensen, O. B. *Acta Chem. Scand.* **1959**, *13*, 900.
(29) Bingham, E. W.; Farrel, H. M., Jr.; Dahl, K. *Biochem. Biophys. Acta* **1976**, *429*, 448.
(30) Alvarez, E. F. *Biochim. Biophys. Acta* **1962**, *59*, 663.
(31) Charton, M. *J. Org. Chem.* **1965**, *30*, 557.
(32) Perrin, D. D.; Dempsey, B.; Serjeant, E. P. "p*K* Prediction for Organic Acids and Bases"; Chapman and Hall: New York, 1981.
(33) Guthrie, J. P.; Cullimore, P. A. *Can. J. Chem.* **1979**, *94*, 240-248. Guthrie, J. P. *Can. J. Chem.* **1979**, *57*, 1177-1185.
(34) Emly, M. Ph.D. Thesis, The Ohio State University, Columbus, OH, 1979.
(35) Emly, M.; Leussing, D. L. *J. Am. Chem. Soc.* **1981**, *103*, 628-634.
(36) Tate, S. S.; Grzybowski, A. K.; Datta, J. *Chem. Soc.* **1964**, 1372.
(37) Hess, J. L.; Reed, R. E. *Arch. Biochem. Biophys.* **1972**, *153*, 225.
(38) Hine, J. *J. Am. Chem. Soc.* **1971**, *93*, 3701.
(39) Cox, R. A.; Smith, C. R.; Yates, K. *Can. J. Chem.* **1979**, *57*, 2952-2959.
(40) Sharma, V. S.; Leussing, D. L. *Inorg. Chem.* **1972**, *11*, 1955-1958.

Table II. Equilibrium Constants

reaction	constant	reaction	constant
	A		
$H_2EP \rightleftharpoons H^+ + HEP^-$	$pK_{1a} = 3.7$ (*a*)	$HEP^- \rightleftharpoons H^+ + EP^{2-}$	$pK_{2a} = 12.0$ (*a*)
$HPYR^{\pm} \rightleftharpoons H^+ + PYR^-$	$pK_a = \sim 5.0$ (*a*)	$OXAC_E^{2-} \rightleftharpoons H^+ + H_{-1}OXAC_e^{3-}$	$pK_a = 12.8$ (34)
$HEP^- \rightleftharpoons PYR^-$	$\log K_{keto} = 5.1$ (13, 21)	$OXAC_E^{2-} \rightleftharpoons OXAC_{1k}^{2-}$	$\log K_{keto} = 0.85$ (34, 35)
vinyl alcohol (HVA) $\rightleftharpoons$ acetaldehyde	$\log K_{keto} = 6.5$ (47)	$HVA \rightleftharpoons H^+ + VA^-$	$pK_a = 11.1$ (33)

ligand	Mg(II)	(ref)	Mn(II)	(ref)	Cu(II)	(ref)
			B. Complex Formation Constants			
EP^{2-}	3.8	(*a*)	5.1	(*a*)	9.0	(*a*)
HEP^-	1.4	(*a*)	2.0	(*a*)	3.4	(*a*)
$HPYR^{\pm}$					0.5	(*a*)
$Hserine^{\pm}$					0.5	(40)
$OXAC_K^{2-}$	0.96	(34)	1.41	(34)	3.1	(34)
$OXAC_E^{2-}$	1.29	(34)	2.11	(34)	5.0	(34)
$H_{-1}OXAC_E^{3-}$	5.7	(34, 35)				
PYR^-	1.1	(*a*)	1.26	(53)	1.43	(52)
OAc^-					1.8	(54)

[a] This work.

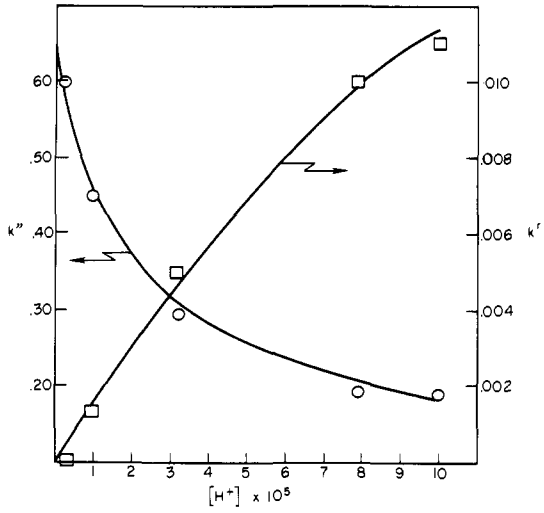

Figure 4. Buffer independent (□) and dependent (○) components of k_{keto}. The solid lines are theoretical.

$HOCH_2CH(NH_3^+)CO_2^-\cdots CU^+$.

Results. A plot of k' vs. $[H^+]$ for the metal ion independent rates, Figure 4, shows that the points fall along a slightly curved line which within the experimental error, passes through the origin. These data indicate the presence of a single kinetically distinguishable pathway which can be written $HEP^- + H^+ \xrightarrow{k_{HEP}^H} PYR^- + H^+$. Using $pK_{1a}^{H_2EP} = 3.7$, a value, $k_{HEP}^H = (1.7 \pm 0.2) \times 10^2$ M^{-1} s^{-1}, was found by fitting the data. The solid line drawn in Figure 4 represents the theoretical curve obtained with these values.

Rate constants for acetic acid and acetate catalysis were resolved by using the relationships

$$k'' = (k_{HEP}^{HOAC} f_{HOAC} + k_{HEP}^{OAC} f_{OAC}) f_{HEP} \quad (10a)$$

$$k'' = (k_{HEP}^{HOAC}[H^+] + k_{HEP}^{OAC} K_a^{HOAC}) K_{1a}^{H_2EP} / ([H^+] + K_{1a}^{H_2EP})([H^+] + K_a^{HOAC}) \quad (10b)$$

where f_{HOAc} and f_{OAC} represent the fractions of total acetate present as free HOAC and OAC^-. The partial conversion of HEP^- to H_2EP at low pH is taken into account by the factor f_{HEP}.

The numerical fit to the k'' data, also shown in Figure 4, yielded $k_{HEP}^{HOAC} = 0.13 \pm 0.04$ and $k_{HEP}^{OAC} = 0.65 \pm 0.03$ M^{-1} s^{-1}. Schellenberger and Hubner[41] have determined the rate constant for the acetate-catalyzed enolization of pyruvate to be 5×10^{-6} M^{-1} s^{-1}. The ratio of the forward to backward rate constants, $0.65/5 \times 10^{-6}$, yields 1.5×10^5 for the ketonization constant, $HEP^- \rightleftharpoons PYR^-$. This value is in good agreement with 4×10^5 reported by Burgner and Ray[42] using the less accurate measurement of the fast uptake of I_2 by concentrated pyruvate solutions.

Scheme I. Path I, Pathway for Apparent General Base Catalysis

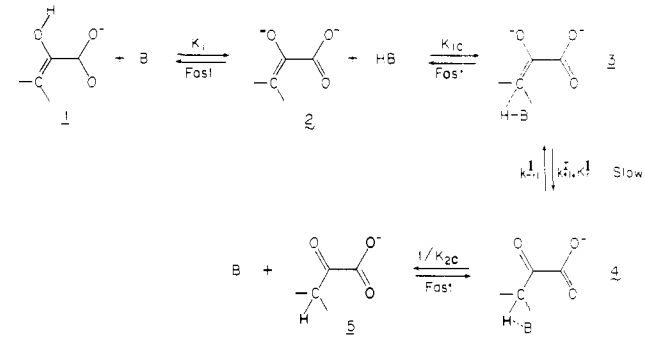

Excess rates arising from metal ion catalysis were found to be linearly dependent on concentrations of all three metal ions studied. Values of k_{keto} for these experiments are presented in Table III. The linearity shows, as expected from the estimates of the $MHEP^+$ stability constants given in Table II, that these complexes are extensively dissociated under the present reaction conditions. The excess rates are buffer-dependent: those for Mg(II) and Mn(II) increase linearly with increasing OAc^- concentration, while those for Cu(II) catalysis decrease. Third-order rate constants (excess rate = $k_{M,HEP}^{OAc}[HEP^-][M][OAc^-]$) of $(9 \pm 1) \times 10^2$ M^{-2} s^{-1} (Mg) and $(4.0 \pm 0.5) \times 10^3$ M^{-2} s^{-1} (Mn) were obtained for the first two metal ions. The Cu(II) data were resolved into terms for $HOAC-CU^{II}$ catalysis, $k_{Cu,hEP}^{HOAC} = (4.7 \pm 0.8) \times 10^5$ M^{-2} s^{-1}, and $^-OAC-CU^{II}$ catalysis, $k_{Cu,HEP}^{OAC} = (3.0 \pm 0.8) \times 10^5$ M^{-2} s^{-1}. The high rate constant for the cooperative Cu^{II}–HOAC-mediated pathway accounts for the inverse pH dependence.

Application of the Marcus Equation to HEP Ketonization. In using eq 1, it is important to correctly identify the rate-limiting step and to convert the value of an experimentally determined rate constant to the value which actually pertains to that step. In some cases, this merely involves dividing an observed bimolecular rate constant by the equilibrium constant for forming the reactant cage complex, which takes into account the work term.[43] In other cases, addition preequilibrium steps must be taken into account. Similarly, it is also necessary to use $\Delta G°$ for the acutal rate-limiting step. In the simplest case, this will merely involve correcting the overall standard free-energy change for the work required to form the reactant and product cage complexes, but here again other equilibrium corrections may need to be made.

The mechanism of ketonization/enolization is considered to involve rate-limiting addition of a proton to, or from, the carbon atom, and fast proton transfer from, or to, the oxygen atom.[15-20]

(41) Schellenberger, A.; Hübner, G. *Chem. Ber.* **1965**, *98*, 1938–1948.

(42) Burgner, J. W., II; Ray, W. J., Jr. *Biochemistry* **1974**, *13*, 4229.

(43) Kreevoy, M. M.; Konasewich, D. E. *Adv. Chem. Phys.* **1971**, *21*, 241.

Table III. Ketonization Rates in the Presence of Metal Ions

Mg(II), M × 10^3	pH[a]	k_{keto} × 10^2 [e] obsd, s^{-1}	k_{keto} × 10^2 calcd, s^{-1}
1.10	4.02	1.1	1.66
2.70	3.97	1.5	2.02
5.30	4.01	1.7	2.62
1.10	4.21	1.4	1.61
2.70	4.21	1.7	2.20
5.30	4.23	2.6	3.18
1.10	4.55	1.5	1.81
2.70	4.54	2.5	2.88
5.30	4.54	4.0	4.61
1.10	4.96	2.3	2.30
2.70	4.96	4.1	4.06
5.30	4.93	7.0	6.72
1.10	5.08	2.5	2.45
2.70	5.09	4.8	4.40
5.30	5.13	8.2	7.70
Mn(II), M × 10^3	pH[a]	k_{keto} × 10^2 obsd, s^{-1}	k_{keto} × 10^2 calcd, s^{-1}
0.20	4.11	1.7	1.54
0.50	4.11	2.0	1.88
1.00	4.11	2.7	2.46
2.50	4.14	4.4	4.32
0.20	4.33	1.5	1.49
0.50	4.35	2.0	2.05
1.00	4.33	2.7	2.93
2.50	4.33	5.0	5.60
0.20	4.48	1.6	1.52
0.50	4.49	2.2	2.23
1.00	4.48	3.2	3.36
2.50	4.48	6.2	6.70
0.20	5.00	2.2	1.87
0.50	5.00	3.3	3.04
1.00	5.00	5.3	4.98
2.50	4.99	11.0	10.6
Cu(II), M × 10^6	10^2 [c] pH[b]	k_{keto} × 10^2 [c] obsd, s^{-1}	k_{keto} × 10^2 calcd, s^{-1}
1.00	4.16	1.9	2.09
3.00	4.14	3.7	3.40
5.00	4.15	5.2	4.69
7.50	4.16	6.8	6.29
15.00	4.18	11.4	11.1
3.00	4.35	2.9	3.20
5.00	4.35	4.1	4.42
7.50	4.34	5.6	5.97
15.00	4.33	9.8	10.6
3.00	5.00	2.7	2.82
5.00	5.02	3.9	3.64
7.50	5.00	4.8	4.70
15.00	4.99	8.6	7.87
3.00	5.60	2.5	2.79
5.00	5.60	3.1	3.45
7.50	5.65	3.8	4.26
15.00	5.63	6.7	6.72

[a] 0.0199 M acetate total. [b] 0.0299 M acetate total. [c] Values of k_{keto} were obtained by fitting numerically integrated curves (eq 5~7) to the experimental curves as described in the text. The relative standard deviations are about 15% of the stated values.

Therefore, apparent general base catalyzed pathways for the ketonization of HEP^- actually have rate-limiting steps involving transfer of a proton from the conjugate acid of the catalytic base to the enolate, EP^{2-}, path I (Scheme I). In general acid catalysis, proton transfer is to the enol, path II (Scheme II).

Paths I and II lead to the rate equations

$$d[PYR^-]/dt = k_{r1}^{I}K_1K_{1C}[HEP^-][B] \quad (11a)$$

$$= k_{HEP}^{B}[HEP^-][B] \quad (11b)$$

$$k_{r1}^{I} = k_{HEP}^{B}/K_1K_{1c} \quad (11c)$$

$$d[PYR^-]/dt = k_{r1}^{II}K_{1C}[HEP^-][HA] \quad (12a)$$

$$= k_{HEP}^{HA}[HEP^-][HA] \quad (12b)$$

Scheme II. Path II, Pathway for General Acid Catalysis

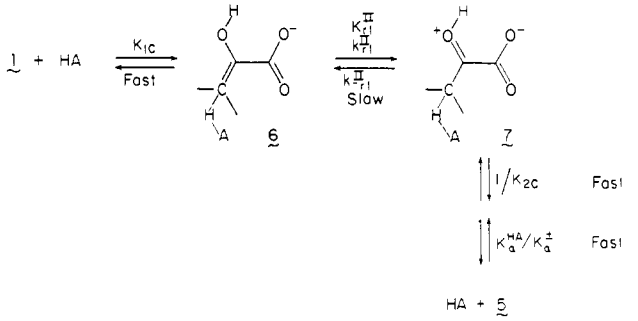

K_1 is obtained from the relationship log $K_1 = pK_a^{HB} - pK_{2a}^{HEP}$, and k_{HEP}^{HA} and k_{HEP}^{B} are the experimentally determined rate constants.

Albery[20] has taken the cage formation constant to be 0.1 M^{-1} for a reaction which involves a neutral species and 1.0 for a "cage" complex involving a molecule of H_2O. We have followed this convention; however, charged species are encountered in the present investigation, and further corrections for charge attraction and repulsion are required. Following the earlier report,[13] the Fuoss equation[44] was employed to make these corrections with the modification that the preexponential term was taken as 0.1, eq 13.

$$K_c = 0.1 \exp\frac{-Z_1Z_2e^2C}{D} \quad (13)$$

$$C = 1/a(1 + \kappa a)$$

$$\kappa = 8\pi e^2I/1000DRT$$

A value of 6 Å for the distance of approach, a, had been found to satisfactorily account for the charge effects.[13]

Kresge[15] has attempted to obtain the work functions for forming the reactant and product cage complexes and $\Delta G^{\ddagger}_0$ by fitting data sets which span large ranges of $\Delta G°$. It was concluded that this approach leads to an underevaluation of $\Delta G^{\ddagger}_0$ and an overestimation of the work term, even though eq 1 is obeyed.[15] The approach employed here possibly leads to an overestimation of $\Delta G^{\ddagger}_0$, owing to the neglect of the work required to rearrange the contact complexes to form the reaction complexes. Kresge has obtained 8 kcal mol for $\Delta G^{\ddagger}_0$,[15] and Toullec[17] reports 10 kcal. Using Albery's conventions, we obtain 13–14 kcal mol^{-1}. Hine[38] and Guthrie[45] employ more detailed calculations which lead to cage formation constants that are about one-sixth those used by Albery.[20] A high degree of correlation between the free energies of forming the cage complexes and the calculated barrier heights exists; nevertheless, regardless of the choice of the work function, at least within reasonable limits, eq 1 is found to be obeyed.

Rate and equilibrium constants for the rate-limiting step for ketonization along path I, **3** → **4**, are given by (11c) and (14).

$$K_{r1}^{I} = K_{keto}/(K_1K_{1c}/K_{2c}) \quad (14)$$

K_{keto} is the overall equilibrium constant for **1** ⇌ **5**.

For path II, the relationships are

$$k_{r1}^{II} = k_{HEP}^{HA}/K_{1c} \quad (15)$$

and

$$K_{r1}^{II} = K_{keto}K_{2c}K_a^{HA}/K_{1c}K_a^{\pm} \quad (16)$$

$K_a^{\pm}$ is the pK_a of the HPYR$^{\pm}$ zwitterion, $CH_3C(CO_2^-)=OH^+ \rightleftharpoons CH_3C(CO_2^-)=O + H^+$.

Cox[46] has proposed that a metal ion may accelerate base-catalyzed enolization of carbonyl compounds by stabilizing the

(44) Fuoss, R. M. *J. Am. Chem. Soc.* **1958**, *80*, 5059.
(45) Guthrie, J. P. *J. Am. Chem. Soc.* **1978**, *100*, 5892 and references cited therein.
(46) Cox, B. G. *J. Am. Chem. Soc.* **1974**, *96*, 6823.

Scheme III. Path III, Metal Ion/General Base Cooperative Pathway

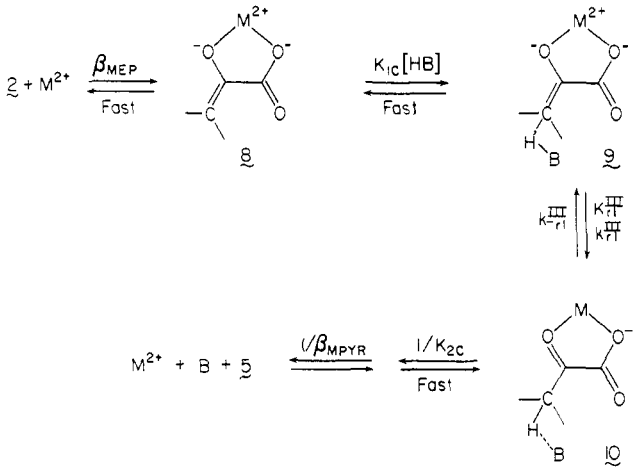

intermediate enolate through complexation. Microscopic reversibility requires that this same interaction facilitate the reverse rate by promoting the loss of a proton from the enol oxygen atom. Owing to the relatively low concentration of the metal ions employed in this study, complexation of HEP^- can be neglected. To initiate reaction along the metal ion dependent pathway, path III (Scheme III), the metal ion is considered to trap the enolate formed through the ionization of the enol. The first-order rate

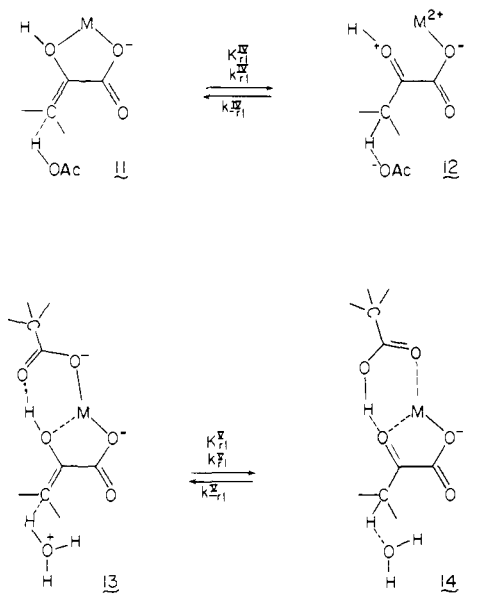

constant for proton transfer in the cage complex, k_{r1}^{III}, is related to the experimentally evaluated third-order rate constant through eq 17. The equilibrium constant is given by eq 18.

$$k_{r1}^{III} = k_{M,HEP}^{B}/K_1K_{1c}\beta_{MEP} \quad (17)$$

$$K_{r1}^{III} = K_{keto}/(K_1K_{1c}\beta_{MEP}/K_{2c}\beta_{MPYR}) \quad (18)$$

Metal ion dependent general acid catalysis involves the reactions of the complexes **9** and **10**:

$$k_{r1}^{IV} = k_{M,HEP}^{HOAC}/\beta_{MHEP}K_{1C} \quad (19)$$

$$K_{r1}^{IV} = K_{keto}K_{2C}\beta_{MHPYR\pm}\beta_{MPYR}K_a^{HOAC}/\beta_{MHEP}K_a^{HPYR\pm}K_{1C} \quad (20)$$

Values of $\Delta G^{\ddagger}$ and ΔG° to be used in eq 1 are obtained from the k_{r1} and K_{r1} defined for the above paths.

The stability constants of the MEP complexes were calculated from the decarboxylation rates of the corresponding MOXAC complexes,[7b] assuming the validity of eq 1. The decarboxylation reaction sequence is

$$M^{2+} + OXAC^{2-} \overset{\beta_{MOXAC}}{\rightleftharpoons} MOXAC, \text{ fast} \quad (21a)$$

$$MOXAC \overset{CO_2}{\rightleftharpoons} MEP\cdots CO_2, \text{slow} \quad (21b)$$

$$MEP\cdots CO_2 \overset{1/K_c}{\rightleftharpoons} MEP + CO_2, \text{ fast} \quad (21c)$$

$$MEP \overset{1/\beta_{MEP}}{\rightleftharpoons} M^{2+} + EP^{2-}, \text{ fast} \quad (21d)$$

The overall equilibrium constant for $OXAC^{2-} \rightleftharpoons EP^{2-} + CO_2$ is 6.8×10^{-7} M.[13] Invoking eq 1, it can be shown that

$$\log \beta_{MEP} = -\Delta G^{\circ}_{CO_2}/1.364 - \log (6.8 \times 10^{-7}) - \log K_c + \log \beta_{MOXAC} \quad (22)$$

where $\Delta G^{\circ}_{CO_2}$ is the smaller root of the quadratic

$$(\Delta G^{\circ}_{CO_2})^2/16\Delta G^{\ddagger}_{o,CO_2} + 0.5\Delta G^{\circ}_{CO_2} + \Delta G^{\ddagger}_{o,CO_2} + 1.364 \log k^{CO_2} - 17.4 = 0 \quad (23)$$

taking $\Delta G^{\ddagger}_{o,CO_2}$ to lie in the range 17.5–18.0 kcal mol^{-1} (see below) and $\log k^{CO_2} = -2.69$ (MgOXAC), −2.24 (MnOXAC), and −0.77 (CuOXAC), the values of $\log \beta_{MEP}$ shown in Table II were calculated. The magnitudes of the constants are consistent with the proposed[6] formation of product complexes having chelate structure **8**.

Support for the use of the $OXAC^{2-}$ decarboxylation rates to obtain the MEP stability constants by way of eq 1 is obtained by simultaneously eliminating the $\log \beta_{MEP}$ from the first-order ΔG° term in the Marcus expressions for both of these reactions.

For base–metal ion cooperative-catalyzed ketonization, eq 1, 17, and 18 yield

$$\Delta G^{\ddagger}_{keto} = -1.364[\log k_{M,HEP}^{B} - \log K_1 - \log K_{1C} - \log \beta_{MEP}] + 17.4 \quad (24a)$$

and

$$\Delta G^{\circ}_{keto} = -1.364[\log K_{keto} + \log (K_{2C}/K_{1C}) + \log \beta_{MPYR} - \log K_1 - \log \beta_{MEP}] \quad (24b)$$

while for decarboxylation

$$\Delta G^{\ddagger}_{CO_2} = -1.364 \log k^{CO_2} + 17.4 \quad (25a)$$

and

$$\Delta G^{\circ}_{CO_2} = -1.364[\log K_{CO_2} + \log K_C + \log \beta_{MEP} - \log \beta_{MOXAC}] \quad (25b)$$

Substituting these expressions into eq 1 (but leaving the quadratic ΔG° terms intact), simultaneously eliminating $\log \beta_{MEP}$, and rearranging leads to eq 26a which expresses the ketonization rate constant as a function of the decarboxylation rate constant.

$$\log k_{M,HEP}^{B} = \log k^{CO_2} + \tfrac{1}{2}(\log \beta_{MPYR} + \log \beta_{MOXAC}) + \tfrac{1}{2}(pK_a^{HB} - pK_{2a}^{HEP}) + A \quad (26a)$$

$$A = \tfrac{1}{2}(\log K_{1c} + \log K_{2c} - \log K_c + 5.10 + 6.16) + (\Delta G^{\ddagger}_{o,CO_2} - \Delta G^{\ddagger}_{o,keto})/1.364 + B$$

$$B = \left[\frac{(\Delta G^{\circ}_{Co_2})^2}{\Delta G^{\pm}_{o\ ,CO_2}} - \frac{(\Delta G^{\circ}_{keto})^2}{\Delta G^{\pm}_{o,keto}}\right] \Big/ (16 \times 1.364)$$

The constants 5.10 and 6.16 are the logarithms of the equilibrium constants for ketonization of HEP^- and addition of CO_2 to EP^{2-}. Except for a second-order correction in the value of B, eq 26a is independent of the value of β_{MEP}. The points (triangles) in a plot of the observed metal ion dependent and independent values of $\log k_{HEP}^{OAC}$ vs. those calculated by using eq 26a, taking $B = 0$, $\Delta G^{\ddagger}_{o,keto} = 13.5$ kcal, and $\Delta G^{\ddagger}_{o,CO_2} = 17.5$ kcal, are seen to fall near to the 45° line in Figure 5. Considering that the range in rate constants spans almost 7 orders of magnitude, the agreement is gratifying.

The results of a more rigorous calculation taking into account β_{MEP}-dependent values of B are plotted as the circles in Figure

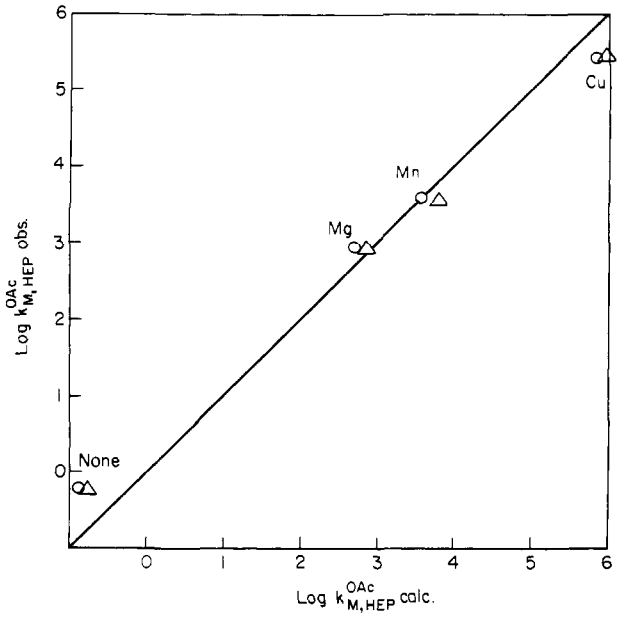

Figure 5. Observed HEP^- ketonization rate constants vs. those calculated from OXAC decarboxylation rates, eq 25a: (△) independent of β_{MEP}, $\Delta G^{\ddagger}_{o,CO_2}$ = 17.5 kcal mol^{-1}; (○) second-order correction for β_{MEP}, $\Delta G^{\ddagger}_{o,CO_2}$ = 18.0 kcal mol^{-1}.

5. In this last calculation, $\Delta G^{\circ}_{CO_2}$ and β_{MEP} were evaluated from eq 22 and 23 and ΔG°_{keto} was obtained by using (26b). The points

$$\Delta G^{\circ}_{keto} = -1.364 \log (K_{keto}) - pK_a^{HB} + pK_a^{HEP} - \log \beta_{MEP} + \log \beta_{MPYR} + \log (K_{1c}/K_{2c}) \quad (26b)$$

are seen to be essentially unchanged from those obtained by the approximate calculation, except that the value of $\Delta G^{\ddagger}_{o,CO_2}$ was increased to 18.0 kcal.

Discussion

Second-order rate constants for the acetate-catalyzed ketonization of HEP^-, acetone enol,[20] and vinyl alcohol[47] are 0.65, 1.7, and 6.8 M^{-1} s^{-1}, respectively. From the results reported in ref 48, the rate constant for the OAc^--catalyzed ketonization of oxalacetate is estimated to be about 0.05 M^{-1} s^{-1}. Replacing the proton of the 1-carbon atom of vinyl alcohol by CO_2^- to give HEP^- causes a decrease of about 1 order of magnitude in the rate constant, and a further decrease of about an order of magnitude results when a proton at the 3-position of HEP^- is replaced by a second CO_2^-. These rate constants are those for the composite reaction, fast transfer of enol proton to base followed by slow proton transfer from the conjugate acid of the base to the enolate carbon atom (path I). The second-order rate constants for the latter step are obtained by dividing the composite constants by the equilibrium constant for the first step:

$$k^{HOAC}_{enolate} = k^{OAC}_{enol}/(10^{pK_a^{HB}} - 10^{pK_a^{enol}})$$

Values of $k^{HOAC}_{enolate}$ are ordered: vinyl alcohol (2×10^7 M^{-1} s^{-1}) ≈ HEP^- (1.5×10^7 M^{-1} s^{-1}) > $OXAC^{2-}$ (7×10^6 M^{-1} s^{-1}). These values span a considerably smaller range than do the composite rate constants, demonstrating that the enol acidities have an important influence on their apparent reactivities.

In Figure 6, values of $\Delta G^{\ddagger}$ calculated from the k_{r1} are plotted against the corresponding ΔG°. Shown are points for general base catalyzed ketonization of (i) HEP^- by acetate; (ii) acetaldehyde enol by various carboxylate anions;[47] (iii) oxalacetate$_{enol}$ by OH^-, PO_4^{3-}, imidazole, diisopropylethanolamine, CO_3^{2-}, and HPO_4^{2-};[13,48,49] and (iv) $MgOXAC_{enol}$ by OAc^-, OH^-, and *N*,*N*,*N*′,*N*′-tetramethylethylenediamine (TN).[13] The solid line has

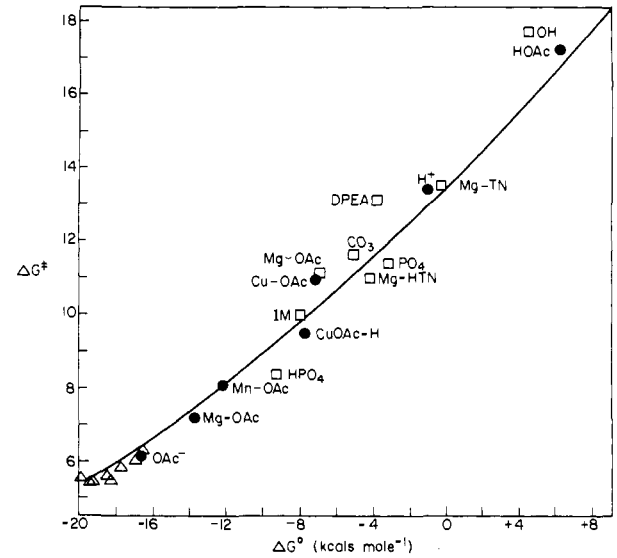

Figure 6. Experimental ketonization barrier heights vs. ΔG_o for the rate limiting step. (△) vinyl alcohol, (●) enolpyruvate, (□) oxaloacetate. DPEA = diisopropropylethanolamine; IM = imidazole; TN = *N*,*N*,*N*′,*N*′-tetramethylethylenediamine.

been calculated from eq 1 taking $\Delta G^{\ddagger}_0$ = 13.5 kcal/mol. It is seen that with only a few exceptions, the points lie within about 0.5 kcal of this line. Catalysis by diisopropylethanolamine toward $OXAC^{2-}$ is seen to yield a higher than predicted barrier, presumably owing to steric hindrance by the amine substituents. The high barrier for apparent OH^- catalysis is commonly observed and is attributed to the low tendency of H^+, H_2O, and OH^- to solvate CH_2.[15-17] A slightly low barrier for HPO_4^{2-} catalysis may arise from the involvement of a proton-switch mechanism.[50]

Points for H^+- and HOAC-catalyzed HEP^- ketonization via path II are also seen to lie along the predicted line. Capon[47] cites evidence that the acid-catalyzed pathway for vinyl alcohol ketonization involves a concerted mechanism, with proton transfer from enol oxygen to a water molecule accompanying addition of a proton to the unsaturated carbon. The large change in the pK_a of the enol oxygen atom as the carbon is protonated satisfies Jencks criteria for a concerted process.[51] Toullec,[17] however, has concluded that the H^+-catalyzed ketonization of acetone enol is not concerted, a view which is supported by Albery's results.[19,20] The difference in mechanism is attributed to the greater stability of protonated acetone relative to protonated vinyl alcohol.[47] Because $HPYR^{\pm}$ is even less acidic than Hacetone$^+$, a concerted mechanism is deemed less likely for the ketonization of HEP^-. This conclusion is consistent with the calculations in which the nonconcerted reaction, **6** → **7**, was assumed.

The third-order rate constants for metal ion–acetate-catalyzed ketonization, $k^{OAc}_{M,HEP}$, increase with increasing affinity of the metal ion for the enolate. Quantitatively, a 300-fold rate increase results when Cu(II), the strongest complex-forming metal ion studied here, replaces Mg(II), the weakest. The metal ion influences the rate along path III in several ways, both favorably and unfavorably. The relationship between the third-order rate constant and the quantities which influence it is expressed by rearranging eq 17, $k^{B}_{M,HEP} = k^{III}_{r1} K_1 \beta_{MEP} K_{1C}$. A quantitative breakdown of the various factors is presented in Table IV for both the metal ion dependent and independent reactions. First, the equilibrium constant for the formal transfer of the enol oxygen proton to acetate, given by the product $K^{III}_1 \beta_{MEP}$, becomes more favorable as the complexing ability of the metal ion increases. The influence of Cu(II),

(47) Capon, B.; Zucco, C. *J. Am. Chem. Soc.* **1982**, *104*, 7576–7572.
(48) Bruice, P. Y.; Bruice, T. J. *J. Am. Chem. Soc.* **1978**, *100*, 4793.
(49) Bruice, P. Y. *J. Am. Chem. Soc.* **1983**, *105*, 4982.
(50) Cunningham, B. A.; Schmir, G. L. *J. Am. Chem. Soc.* **1966**, *88*, 551. Hogg, J. L.; Jencks, D. A.; Jencks, W. P. *J. Am. Chem. Soc.* **1977**, *99*, 4772–4778.
(51) Jencks, W. P. *J. Am. Chem. Soc.* **1972**, *94*, 4731–4732; *Acc. Chem. Res.* **1980**, *13*, 161–169.
(52) Raghavan, N. V.; Leussing, D. L. *J. Ind. Chem. Soc.* **1977**, *54*, 68–73.
(53) Schultz, D. C.; Leussing, D. L. *J. Am. Chem. Soc.* **1964**, *86*, 4846.

Table IV. Acetate-Catalyzed Ketonization of Enolpyruvate

$$M^{2+} + HEP^- + B^{i-} \xrightleftharpoons{K_1\beta_{MEP}} MEP + HB^{1-i}$$

$$MEP + HB^{1-i} \xrightleftharpoons{K_{1C}} MEP\cdots HB^{1-i}$$

$$MEP^+\cdots HB^{1-i} \xrightleftharpoons{K_{r_1}} MPYR^+\cdots B^{i-}$$

$$MPYR^+\cdots B^{i-} \xrightleftharpoons{1/K_{2C}} MPYR^+ + B^{i-}$$

$$MPYR^+ \xrightleftharpoons{1/\beta_{MPYR}} M^{2+} + PYR^-$$

M^{2+}	$\log k^{OAC}_{M,HEP}$	$\log (K^{III}_1\beta_{MEP})$	K_{1C}, M^{-1}	K_{2C}, M^{-1}	$\log K^{III}_{r_1}$	$k^{III}_{r_1}$, s^{-1}
none	−0.19	−7.35[a]	0.10	0.055	12.2[b]	1.4×10^{8} [c]
Mg	2.95	−3.55	0.10	0.21	10.4	3.2×10^{7}
Mn	3.60	−2.25	0.10	0.21	8.9	7.1×10^{6}
Cu	5.48	1.65	0.10	0.21	5.2	6.8×10^{4}

[a] $\log K_1 = pK_a^{HOAc} - pK_a^{HEP}$. [b] $\log K^{I}_{r_1}$. [c] $k^{I}_{r_1}$.

for example, is to increase this proton-transfer constant by a factor of $10^{9.0}$ over that which pertains to the metal ion independent reaction, K^1_1.

Second, the equilibrium constant for transfer of a proton from acetic acid to enolate carbon (K^1_{r1} and K^{III}_{r1}) decreases when a metal ion is bound to the enolate and continues to show a decrease as the complexing ability of the metal ion increases. A decrease by a factor of 10^7 results when EP^{2-} is complexed to Cu(II). According to eq 18, K^{III}_{r1} depends on the ratio β_{MPYR}/β_{MEP}, and not only are the stabilities of the enolate complexes higher than those of the pyruvate complexes, but the enolate stabilities also show a larger dependence on the nature of the metal ion. It is this last property which determines the inverse trend in the K^{III}_{r1} toward increasing binding power of the metal ion.

According to eq 1, a decrease in the value of K^{III}_{r1} yields a lower k^{III}_{r1}. Because the quadratic term in $\Delta G°$ is small and the linear term possesses a multiplier of $^1/_2$, changes in the rate constant roughly approximate the square root of the changes in the equilibrium constant. The preequilibrium constants for enol ionization are directly proportional to β_{MEP}, while the first-order rate constants show a rough inverse dependence on the square root of β_{MEP}, neglecting small changes in the β_{MPYR}. The third-order rate constants for cross metal ion–acetate catalysis are therefore predicted to depend on $\beta^{0.5}_{MEP}$. The experimental results are consistent with this conclusion.

Changes in the reactant and product cage complexes have relatively small effects on the reaction rates. To a first approximation, K_{1C} is independent of whether or not EP^{2-} is bound to a metal ion, owing to the absence of a charge on the acetic acid molecule. In contrast, K_{2C} becomes more favorable when EP^{2-} is complexed to a divalent metal ion: of the two proton transfers, $EP^{2-}\cdots HOAC \rightarrow PYR^- \cdots OAc^-$ and $MEP\cdots HOAc \rightarrow MPYR^+\cdots OAC^-$, the former tends to be slowed by electrostatic repulsion between the products, but charge attraction tends to increase the rate of the latter.

Cooperativity between HOAC and Cu(II) in HEP^- ketonization is surprisingly effective, showing a rate constant higher even than that observed for Cu(II) and OAc^-. This reactivity furnishes an example of the use of eq 1 as an aid in selecting the more likely pathway from two alternatives. In a direct proton transfer from HOAC to the unsaturated carbon atom of complexed HEP^-, **11** → **12**, Cu(II) stabilizes the reactant, $Cu(HEP)^+$, relative to the product, $[Cu(CH_3C(CO_2^-)=OH^+)]^{2+}$. Qualitatively, complexation is therefore expected to slow the rate of ketonization. Quantitatively, when eq 1 is used, the third-order rate constant for the direct attack of HOAC on $Cu(HEP)^+$ is predicted to be about 70 M^{-2} s^{-1}, which is in serious disagreement with the observed value of 4.7×10^5 M^{-2} s^{-1}. An alternative pathway indistinguishable with respect to the rate law is one in which H^+ attack occurs on the enolate carbon atom in the mixed-ligand complex, $(HEP)Cu^{II}(OAc)$, concerted with transfer of the enol oxygen proton to the complexed OAc^-, **13** → **14**. The predicted rate constant for this latter route, 1.1×10^5 M^{-2} s^{-1}, is close to the observed result. These calculations are based on rough estimates of the stability constants of $Cu(HEP)^+$ and $Cu(HPYR^{\pm})^{2+}$; nevertheless, the substantial difference obtained between the calculated rate constants for the two postulated reaction routes demonstrates that useful conclusions regarding likely and unlikely reaction paths may be drawn from even approximate calculations. The point representing the concerted pathway is shown in Figure 6 as the closed circle designated as Cu(OAc)–H. This point is seen to lie near the theoretical line. Here, the metal ion further aids the reaction by bringing a base near to the enol oxygen proton. Because many complexing metal ions are hydrolyzed in solutions near neutral pH, analogous pathways involving proton transfer to coordinated OH^- may account for the relatively strong apparent solvent-catalyzed pathways observed in the enolization of metal–$OXAC^{2-}$ complexes.[7b]

Registry No. 1, 19071-34-2; HKPEP, 4265-07-0; NaPYR, 113-24-6; H_2PEP, 138-08-9; $HPEP^-$, 67533-04-4; PYR^-, 57-60-3; Mg(II), 22537-22-0; Mn(II), 16397-91-4; Cu(II), 15158-11-9; OAc^-, 67057-47-0; HOAc, 64-19-7.

(54) Yasuda, M.; Yamasaki, K.; Ohtaki, H. *Bull. Chem. Soc. Jpn* **1960**, *23*, 1067.